Article

Effect of Volume Fraction and Temperature on Dielectric Relaxation Spectroscopy of Suspensions of PS/PANI Composite Microspheres

Mingjuan Han, and Kongshuang Zhao

J. Phys. Chem. C, **2008**, 112 (49), 19412-19422 • Publication Date (Web): 14 November 2008

Effect of Volume Fraction and Temperature on Dielectric Relaxation Spectroscopy of Suspensions of PS/PANI Composite Microspheres

Mingjuan Han and Kongshuang Zhao*

College of Chemistry, Beijing Normal University, Beijing 100875, China

Received: April 23, 2008; Revised Manuscript Received: October 6, 2008

In this work, we aim to contribute new data on the dielectric relaxation behavior of suspensions of nonconducting/conducting composite microspheres (polystyrene/ polyaniline, PS/PANI). Then, the dielectric investigation over the frequency range of 40 Hz to 110 MHz has been carried out to display the characteristic of dielectric relaxation spectroscopy of suspensions with PS/PANI composite microspheres from two contributions which are the dependences of dielectric relaxation spectroscopy of suspensions on the volume fraction of particles (ϕ) and temperature (T), individually. Two relaxations can be identified in dielectric spectroscopy of suspensions: the so-called α- relaxation (typically at kHz) due to the polarization of counterions, and the Maxwell−Wagner−O'Konski (M−W−O) relaxation (typically at MHz) ascribed to a consequence of an accumulation of polarized charges on the boundary surfaces of the dispersed particles. The dependences of dielectric parameters by fitting data with Cole−Cole equations on ϕ and T have been discussed in detail, respectively. According to the dielectric analysis, several interesting phenomena arise in the range of investigation: First, special dielectric increments, where $\partial\varepsilon_l = (\varepsilon_l - \varepsilon_m)/\phi$ and $\partial\varepsilon_h = (\varepsilon_m - \varepsilon_h)/\phi$ denoting the low- and high-frequency relaxation amplitude of suspensions of PS/PANI particles per unit volume, respectively, are increasing with the enhancement of volume fraction ϕ. Second, all high-frequency permittivities (ε_h) are higher or much higher than the permittivity of aqueous solution (80.05 at 18 ± 1 °C). On the basis of the comparisons between PS/PANI and PS, PS/PPY, PS/ZnO particles, we extract some proposals to responsible for such interesting phenomena, namely, except for the two distinct relaxations, α-relaxation and M−W−O relaxation, suspension exhibits an additional dielectric relaxation over the megahertz frequency range, due to the polarization of internal double layer of the thin layer of conducting polymer PANI when an external field is employed. Meanwhile, the different dependences of ε_h on ϕ for suspensions of PS/PANI (PS/PPY) and PS/ZnO particles are ascribed to the different conducting mechanism and surface morphology of conducting polymer PANI (PPY) and ZnO shells. Finally, after the detailed analysis we obtained the activation energy E_a of the low- and high-frequency relaxations of suspensions of PS/PANI microspheres which is experimentally determined by the dielectric data, individually.

1. Introduction

Polyaniline[1,2] is an electrically conducting polymer with many features that could be exploited in various applications. [3−5] But its main disadvantages are poor processability both in melt and solution due to its stiffness of the backbone. [6] The preparation of particles with controlled core−shell morphology is one of the ways to improve the processibility of this polymer and to obtain electrically conducting composites. The particles with typically well-defined structure have increasingly attracted interest due to their potential applications in photonic crystals, multienzyme biocatalysis, and drug delivery systems. [7] Particularly, the fabrication of polystyrene (PS) cores coated with inherently conducting polymers (ICPs),[8] such as polypyrrole (PPY),[9] polyaniline (PANI),[10] and polyethylene-dioxythiophene (PEDOT),[11] has been investigated. This extensive upswing of the passion on these studies is not only because it is capable of improving the processability of conducting polymer materials, but also because of the attractive properties of these materials such as well-defined colloidal dimensions or morphologies,[2] biocompatibility,[12] high surface area, efficient radiation adsorption, good film-forming properties,[13] wide spectrum of surface functionalization.[14]

Despite a massive amount of work on the synthesis, characterization and application of PS particles coated with conducting polymer shells, as we known that suspensions of particles have found applications in innumerable technological fields, it is mostly concentrated systems that are of interest in the large-scale production of goods ranging from common foods to controlled drug release devices. Correspondingly, no matter what the concentration of solids is, most properties of colloidal suspensions, such as notably their stability, flow behavior and electrical property are controlled by the structure and electrical state of the solid /liquid interface and its ionic atmosphere (named electrical double layer, EDL hereafter). [15−18] As we known that dielectric spectroscopy of colloid dispersions is a powerful and promising tool for the precise characterization of the electrical property of interfaces. Over the last three decades, knowledge of such dielectric behavior of the systems (PS) has taken much benefit from dielectric techniques, for example, the frequency behavior of the dielectric properties of aqueous suspensions of charged spherical monodispersed particles has been widely studied experimentally,[19−23] theoretically [24−28] and numerically.[18,29,30] Most of these studies deal with the dependence of the dielectric spectra of suspensions of polystyrene

* To whom correspondence should be addressed. E-mail: zhaoks@bnu.edu.cn.

10.1021/jp803530m CCC: $40.75
Published on Web 11/14/2008

particles on the particle size, particle concentration, particle charge, electrolyte concentration, and pH.

All the reports show that dielectric spectroscopy is one of the most sensitive and powerful tool for understanding the influence of ions on the segmental and local motions as well as the information on the electrokinetics of particles. The deviation from equilibrium state for the ion atmosphere around particles leads to relaxation phenomena, with characteristic relaxation frequency typically from kHz to MHz, which means that dielectric behavior of particles suspended in aqueous electrolyte solutions is characterized by two relaxation regions which are the most sensitive to the dynamics of the electric double layer of interfaces.[15,31]

However, the study of dielectric relaxation on simple and well-defined colloid systems (nonconducting core coated with the conducting shell) including experimental and theoretical investigations is so few up to now except for our own attempt on the dielectric study of suspensions of PS/PPY[32] and PS/ZnO[33] composite microspheres. Meanwhile, dielectric study on this system has proven to be challenging since heterogeneous systems, in particular aqueous suspensions of such colloid particles, are very complex systems characterized by a variety of dynamic processes, occurring at different time scales, which involves characteristic of the complex interfacial structure of both dispersed particles and disperse medium. Therefore, in order to gain excellent understanding of such suspensions, a series of dielectric measurements should be carried out on such well-defined systems. Here, in order to further understand and characterize such practical systems, and expand experimental database or theoretical reference in anticipation of future modeling study of dielectric relaxation spectroscopy, it is necessary to model the ionic distribution and dynamics in the EDL for PS/PANI suspensions.

Therefore, as an extension of the previous work carried out by our group, the dielectric measurement of suspensions of PS/PANI core−shell microspheres has been carried out over the frequency range from 42 Hz to 110 MHz. The aim of this work is to show new data on the dielectric relaxation spectroscopy of suspensions of PS/(conducting polymer) composite microspheres from two contributions—the act of volume fraction and temperature on dielectric behaviors of suspensions of PS/PANI composite microspheres, individually. The analysis of this work is guided by the dielectric parameters fitted by Cole−Cole equation. Special emphasis is placed on the characteristic of dielectric relaxation of suspensions of PS/PANI microspheres and we further analyze on the mismatch of dielectric relaxation behavior between the nonconducting/conducting (PS/PANI, PS/PPY and PS/ZnO) core−shell composite particles and classical particles-PS, then use the present manuscript as an opportunity to briefly highlight any differences or similarities between these closely related systems. Finally, we have discovered that the dielectric behavior of PS/PANI microspheres is much different with that of suspensions of the classical PS particles. Facing each dielectric characteristic of suspensions of PS/PANI composite particles, we elucidated it in detail on the basis of comparing PS/PANI composite particles with PS/PPY (PS/ZnO) composite particles and the classical particles PS, one by one. Finally, we concluded that the thin layer of conducting PANI (PPY) shell and the roughness of surfaces are responsible for the special dielectric behaviors of such PS/PANI (PS/PPY) core−shell model complex system.

2. Experimental Section and Methods

2.1. Particle Suspensions. The samples investigated in this work were suspensions of monodisperse spherical PS/PANI particles with about 1um radii, which were fabricated by means of previous report.[34] SEM image of the PS/PANI composite microspheres was shown in Figure 1. The dissociation of ionic groups stemming from the surface of particles themselves would happen when the PS/PANI particles were dispersed into the distilled water. Therefore, the samples were purified with distilled water to remove adsorbing ions on the surface of particles using the dialyzing method until the conductivity of supernatant was around 1×10^{-6} S/m, in order to know the electrical double layer, precisely.

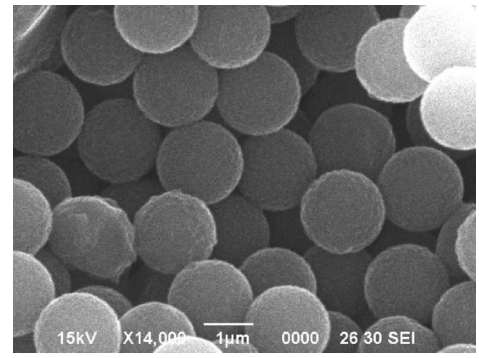

Figure 1. SEM image of PS/PANI composite microspheres.

First, we collected the samples by using the high-velocity centrifugal machine and a green power (PS/PANI) was obtained after being dried in a vacuum oven at 30 °C, then, the green power (PS/PANI) redispersed in distilled water at a maximum volume fraction up to 30% approximately. The determination of maximum volume fraction of particles was as following: a given amounts of PS/PANI particles were dispersed in 20 mL measuring cylinder which loaded with 8 mL distilled water and sonicated for 30 min to disperse any coarse aggregates. Then, approximately defined as $\phi_{Tem} \approx (V_p)/(V_p + V_m) \approx (V_p)/(V_{totle}) \approx (V_{totle} - 8)/(V_{totle})$, where ϕ_{Tem} is the volume fraction occupied by the particles in the suspension, V_p and V_m are the volumes of particles and medium, separately. Finally, the above concentrated suspension (vol % ≈ 30%) determined by the method above was diluted with 0.05 mM KCl electrolyte solution step by step, then, suspensions of particles with different volume fractions were gained, which was presented in Section 3.2. Second, the above concentrated suspension (vol % ≈ 26.5%) was extracted for the dielectric measurement of suspensions of PS/PANI microspheres dispersed in different temperatures (from 0 to 60 °C), just as shown in Section 3.3.

Prior to each dielectric measurement, each of PS-PANI suspensions was sonicated for 15 min to disperse any coarse aggregates that may have formed on long standing. This was particularly necessary for suspensions with higher particle volume fraction.

2.2. Dielectric Measurement. Dielectric measurements were carried out in frequency range from 40 Hz to 110 MHz on an HP 4294A with Precision Impedance Analyzer (Agilent Technologies) tested and calibrated in accordance with the procedure recommended by the manufacturer, controlled by a personal computer. The amplitude of the applied alternating field was 500 mV, and the measurement temperature was 18 ± 1 °C. The dielectric measurement cell with concentrically cylindrical platinum electrodes was employed, which has been described and used in previous works.[35,36] The solution volume used in the experiment was 2 mL in order to submerge the electrodes. Prior to the transformation, all experimental data were subjected to certain corrections[37] for the errors arising from measuring cell. First, the experimental data were corrected by the stray

capacitance C_r and cell constant C_l of the permittivity cell, which were determined by using several standard liquids, such as pure water, ethanol and acetone. The residual inductance L_r due to the cell assembly and the terminal leads will make errors, so L_r of the dielectric cell was determined by use of standard KCl solutions with different concentrations. Then the permittivity and conductivity were calculated from the corrected capacitance and conductance based on eqs 1−4

$$C_s = \frac{C_x(1+\omega^2 LrC_x) + LrG_x^2}{(1+\omega^2 LrC_x)^2 + (\omega LrG_x)^2} - Cr \quad (1)$$

$$G_s = \frac{G_x}{(1+\omega^2 LrC_x)^2 + (\omega LrG_x)^2} \quad (2)$$

$$\varepsilon = \frac{C_s - C_r}{C_l} \quad (3)$$

$$\kappa = \frac{G_s \varepsilon_0}{C_l} \quad (4)$$

Where C_x, G_x, C_s, and G_s are the measured and corrected capacitance and conductance, respectively, $\omega(=2\pi f)$ is the angular frequency, ε_0 is the permittivity of vacuum equal to 8.8541×10^{-12} F·m^{-1}, and ε and κ are the calculated permittivity and conductivity, respectively.

2.3. Determination of Dielectric Parameters from Dielectric Spectra. Dielectric measurements of suspensions of PS/PANI particles were carried out in the frequency range from 40 Hz to 110 MHz on an HP 4294A with Precision Impedance Analyzer, then the experimental data (permittivity and conductivity changing with frequency) were obtained. After the confirmation of two dispersions for the system, the Cole−Cole formula (eq 5) of the two-dispersion terms is used to fit the experimental data of two-dispersion systems to obtain the dielectric parameters,[38]

$$\varepsilon^* = \varepsilon_h + \frac{\varepsilon_l - \varepsilon_{mid}}{1+(j\omega\tau_l)^{\beta_l}} + \frac{\varepsilon_{mid} - \varepsilon_h}{1+(j\omega\tau_h)^{\beta_h}} + \frac{\kappa_l}{j\omega\varepsilon_0} + A\omega^{-m} \quad (5)$$

where ω is the angular frequency and ε_0 is the permittivity of vacuum. τ_l and τ_h are the relaxation time of the low- and high-frequency relaxations, respectively. β_l and β_h are the parameters indicating the distribution of relaxation time τ_l and τ_h, individually. A and m in the electrode polarization term are adjustable parameters. In our case, the real part and conductivity part of eq 5 are fitted to experimental data to obtain the dielectric parameters, meanwhile, the peak of dielectric loss is used to judge the position of occurrence of dielectric relaxation.

It should be pointed out that the limiting conductivity values of high-frequency κ_h and middle-frequency that κ_{mid} cannot be obtained from the above equation. Therefore, κ_h is estimated from the equation,[39]

$$\kappa_h = ((\varepsilon_{mid} - \varepsilon_h)) \times 2 \times \pi \times f_0 \times \varepsilon_0) + \kappa_{mid} \quad (6)$$

and κ_{mid} is determined from the plot of conductivity using the single Cole−Cole equation to fitting the experimental data based on the obtained dielectric parameters (i.e., ε_m, ε_h, β_h, f_h). The best-fitting dielectric parameters, obtained by fitting the experimental data with the Cole−Cole equation (eq 5), are displayed in Sections 3.2 and 3.3. And κ_l are determined by using equation $\kappa = \omega\varepsilon_0\varepsilon'' + \kappa_l$[40] to fit the experimental data of conductivity on the basis of the dielectric parameters (i.e., ε_l, ε_h, β, f_0) earlier obtained from the curve-fitting of eq 5 to experimental data. All the values β are around 0.85−0.95 in our best-fitting results, indicating that the dielectric relaxation are closer to the Debye-type relaxation.

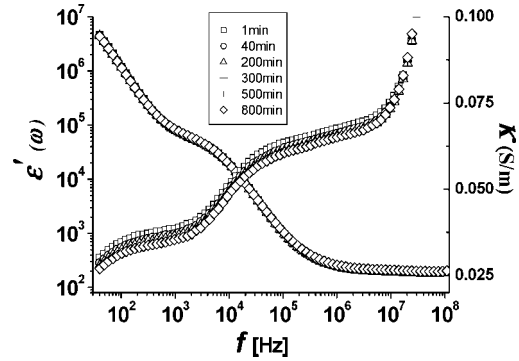

Figure 2. Data of dielectric measurements of suspensions of PS/PANI from 1 to 800 min.

3. Results and Discussion

3.1. Dependence of Dielectric Behavior of Suspensions of PS/PANI Microspheres on the Measuring Time. The dielectric measurement is sensitive to the stability of suspensions of PS/PANI mirospheres, therefore, it is carried out in every 20 min controlled by a computer program to test the stability of suspensions. Then we extract some results of the dielectric measurements of suspensions of PS/PANI microspheres from 1 to 800 min as shown in Figure 2. Here, we should point out that within 40 min both the permittivity and conductivity of suspensions show no changing, which indicates that the good stability of suspensions of PS/PANI can be remained within 40 min, meanwhile, it means that suspensions of PS/PANI particles are stable and the dielectric measurement can be reproduced within such time range. Therefore, we can lose focus on the effect of stability of suspensions in our consequent investigation of Sections 3.2 and 3.3 on the dielectric behaviors of suspensions of PS/PANI microspheres since each dielectric measurement can be finished only within 1−2 min.

As can be seen from Figure 2, the permittivity of each suspension does not vary with the measuring time, furthermore, its conductivity shows obvious decrement within 800 min. This phenomenon will be explained in detail in the following: As we well-known that the particles in suspensions will go down due to the gravity of microspheres, it means that the volume fraction of particles between two electrodes is decreasing with the increment of the measuring time since a few particles will go down to the floor of measuring cell, then it indicates that the low dielectric constant material (PS/PANI) is substituted by high dielectric constant material (water). According to the Maxwell−Wagner equation,[41] the permittivity of suspensions is composed of two contributions from disperse phase and disperse medium, therefore, the decrement of few low dielectric constant material (PS/PANI) can not result in the obvious change of permittivity of suspensions since the permittivity of disperse medium(aqueous solution) is much larger than disperse phase. Otherwise, compared with the permittivity of suspensions, the conductivity of suspensions shows different dependence on contributions from disperse phase and disperse medium. The reason for this is the conductivity of particles is much higher than that of aqueous solution, which is ascribed to the surface conductivity of particle due to the presence of the electrical double layer around a particle, and it can be confirmed when we trace back the M−W−O interfacial polarization theory. [42] Accordingly, the conductivity of suspensions is much sensitive to component of suspensions than the permittivity.

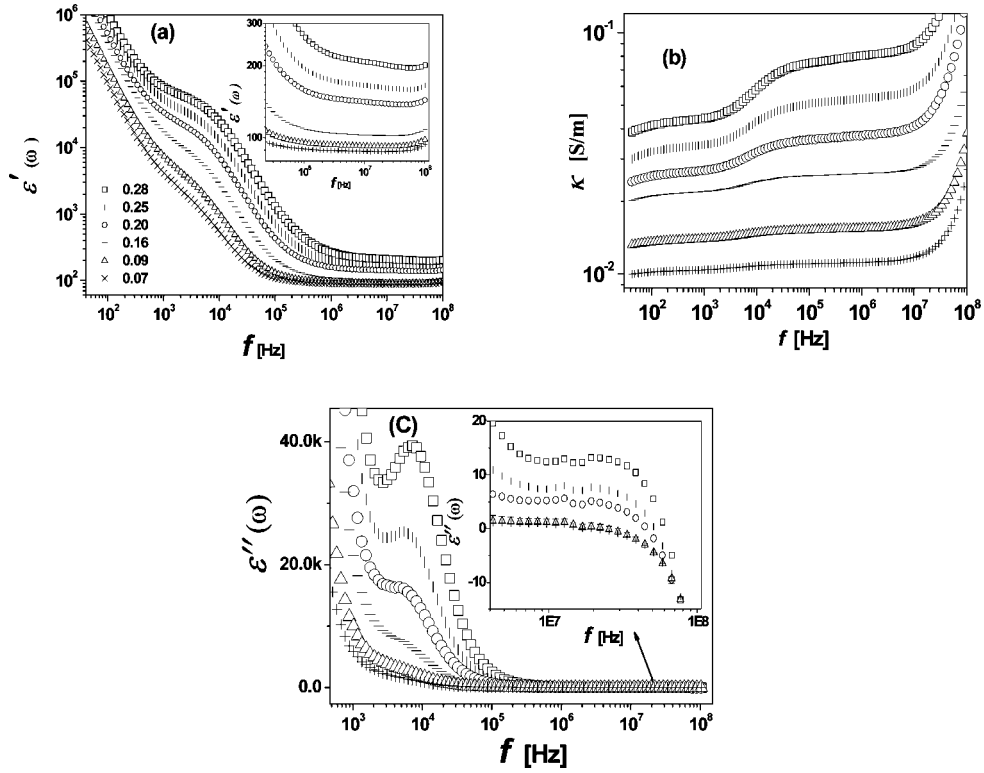

Figure 3. Frequency dependency of (a) permittivity ε' and (b) conductivity κ and (c) dielectric loss ε'' spectrum for suspensions of PS/PANI core−shell microspheres with different volume fractions as indicated. Note: the same symbols are all the same meanings.

All in all, the dielectric measurement of suspensions of PS/PANI particles has been investigated and used to detect the stability of suspensions of PS/PANI particles.

3.2. Dielectric Relaxation of Suspensions of PS/PANI Particles with Different Volume Fractions Dispersed in KCl Electrolyte Solution. Figure 3 shows the frequency dependence of the permittivity and conductivity for suspensions of PS/PANI core−shell particles with different volume fraction (from 0.28 to 0.07) over the frequency range from 42 Hz to 110 MHz. Two dielectric relaxations are displayed by the spectrum of permittivity ε' in Figure 3a, and confirmed by two peaks represented by the spectrum of dielectric loss $\varepsilon''(\omega)$ in Figure 3c. The dielectric loss $\varepsilon''(\omega)$ is presented by the logarithmic derivative $\varepsilon''_D(\omega) = -(\pi/2)(\partial\varepsilon'/\partial \ln \omega)$ on the basis of the logarithmic derivative of raw $\varepsilon'(\omega)$ data ($\varepsilon'(\omega)$ is the real part of the permittivity of the suspensions for a frequencyω of the applied AC field), which shows an excellent representation of the true imaginary part of the permittivity, $\varepsilon''(\omega)$, and turns out to be very effective in resolving overlapped relaxations. [18,43,44] Therefore, two distinct characteristic relaxations—the low- and high-frequency relaxations occurred at kilohertz and megahertz frequencies, respectively, are distinguished in Figure 3c.

The abrupt increments of both permittivity below kHz and conductivity above MHz are considered to be caused by the electrode polarization due to the accumulation of spatial charges on the electrode surface, otherwise, this phenomenon is not our expectation since it often covers the low-frequency relaxation (α-relaxation) in the permittivity spectrum and covers the high-frequency relaxation (M−W relaxation) in the conductivity spectrum. A typical and clear result of the elimination of electrode polarization effect is shown in Figure 4, the data in which are extracted from the experimental data (vol % ≈ 0.28) of Figure 3. As shown in Figure 4, the section circled by ellipse is the comparison between the experimental data and the data of eliminating electrode polarization from the experimental data.

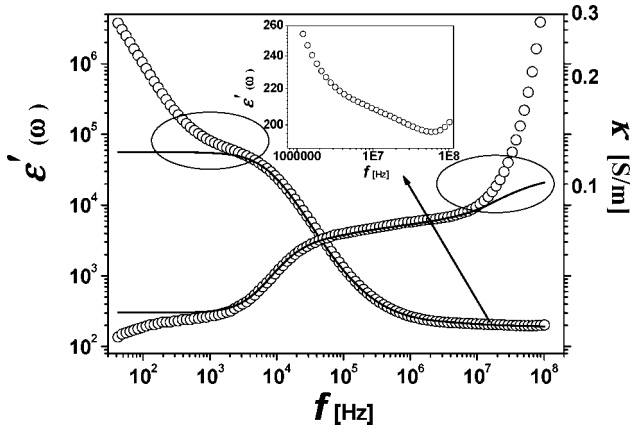

Figure 4. Comparison between the experimental data (○) of suspensions of PS/PANI particles and the fitting curve (—) after eliminating the electrode polarization.

Then, from the conductivity spectrum around 10^7 Hz we disclose the second relaxation—so-called M−W relaxation, which has been considered in permittivity spectrum just as shown in the iconograph of Figure 4. Meanwhile, from the permittivity spectrum we find that the abrupt increment of permittivity below kHz has been eliminated from the experimental data. Therefore, all results show that the precise dielectric parameters can be obtained after eliminating the effect of electrode polarization.

Here we should point out the permittivity of the low-frequency relaxation is still high ($\sim 5 \times 10^4$) as shown in the fitting curve of low-frequency data in Figure 4. Otherwise, this behavior is not unexpected, the reason for this is the length scale of the induced dipole originated from the magnitude of particle with 1um radius is much larger than a molecular dipole, so which results in this large permittivity of the low-frequency relaxation. The early theory attributes the large permittivity to the polarization of counter-ions mobile associated with the fixed

TABLE 1: Dielectric Parameters of Suspensions of PS/PANI Core−Shell Microspheres with Different Volume Fractions Dispersed in 0.05 mM KCl Electrolyte Solution[a]

	dielectric parameters							
volume fraction (ϕ)	ε_l	ε_m	ε_h	$\Delta\varepsilon_l$	$\Delta\varepsilon_h$	κ_l (S/m)	τ_l [s] ($\times 10^5$ s)	τ_h [s] ($\times 10^9$ s)
0.28	56541	204	192	56337	12	0.0453	1.9493	8.2769
0.25	32541	163	155	32378	8	0.0339	2.2162	7.2283
0.20	21040	141	134	20899	7	0.0266	2.5732	7.2283
0.16	10139	103	101	10036	2	0.0218	2.9555	6.2892
0.09	4043	91	90	3952	1	0.0139	2.9582	5.4707
0.07	2614	88	87	2526	1	0.0104	3.2548	5.4520

[a] $\Delta\varepsilon$ and $\Delta\kappa$ are the permittivity and conductivity increments, defined as $\Delta\varepsilon_l = \varepsilon_m - \varepsilon_l$; $\Delta\kappa_l = \kappa_m - \kappa_l$ and $\Delta\varepsilon_h = \varepsilon_h - \varepsilon_m$; $\Delta\kappa_h = \kappa_h - \kappa_m$, respectively.

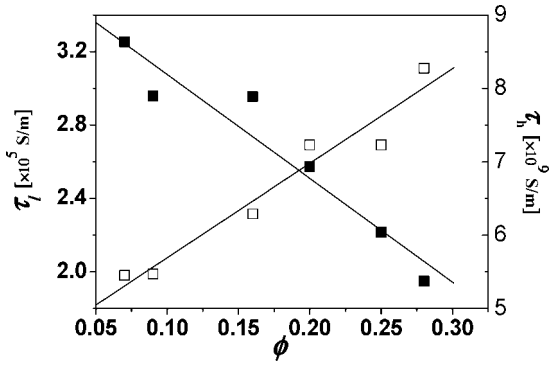

Figure 5. Dependence of relaxation time of low- (■) and high-frequency (□) relaxations on the volume fraction of particles, individually. The lines are the linear fitting results of experimental data.

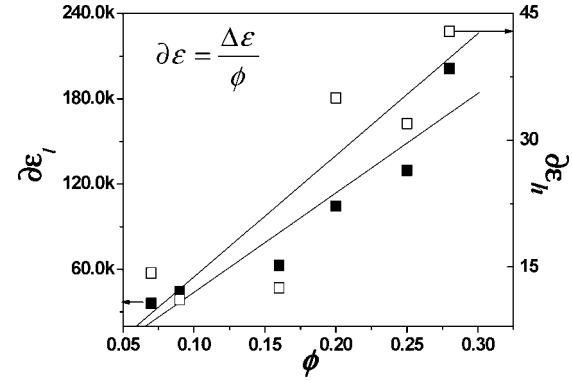

Figure 6. Plot of the special dielectric increments of the low- (■) and high-frequency (□) relaxations for suspensions of PS/PANI particles as a function of the volume fraction ϕ. The lines are the linear fitting results of experimental data.

surface charge of particles,[19,45] then, later work focused it on the electric double layer polarization by electrokinetic processes,[24] no matter which explanation both of them will result in the appearance of the low-frequency relaxation. The relaxation at high frequencies, hereafter named the high-frequency relaxation, is originated from the famous M−W effect,[41,46] typically occurring at the frequency range of megahertz, then extended by O'Konski[42] by introducing the concept of surface conductivity.

According to the determination of dielectric parameters and the description of eliminating electrode polarization in Section 2.3, we use the valid empirical equation, namely, the Cole−Cole formulas with two dispersion terms and electrode polarization term, to fit the experimental data, then the dielectric parameters are obtained and best-fitting results are listed in Table 1.

Table 1 shows the dielectric parameters of suspensions of PS/PANI core−shell microspheres with different volume fractions (from 0.07 to 0.28) dispersed in 0.05 mM KCl electrolyte solution. As is known, dielectric parameters represent the collective property of suspension, therefore, the dependences of dielectric parameters on the volume fraction will be discussed in detail in the following paragraphs for further investigation.

3.2.1. Dependence of the Characteristic Relaxation Time on the Volume Fraction. In the frequency range under our investigation, the dielectric spectroscopy of suspensions of PS/PANI core−shell microspheres is characterized by two distinct relaxations, here we omit the calculation of the low- and high-frequency relaxation times since it has been illustrated in detail in our previous works.[32,33] For further investigation on the dielectric behavior of suspensions of PS/PANI microspheres, plot of the characteristic relaxation time given in Table 1 against the volume fraction (ϕ) is shown in Figure 5. It can be observed that the low-frequency relaxation time (τ_l) decreases, otherwise the high-frequency relaxation time (τ_h) increases with the increment of ϕ, monotonically. The former is in accordance with the prediction of the classical volume diffusion mechanism (VDM) about the relaxation of concentration polarization employed by Shilov and Borkovskaya [47,48] and the latter shows an agreement with the prediction of the M−W relaxation at high-frequency regime. [24] As for detail about the analysis, the correspondence references [32,33] can be referred, the aim of this analysis is to display that the low-frequency relaxation process is dominated by VDM for suspensions of PS/PANI particles under our investigation. It means that the exchange of counterions in the Stern layer with the free ions in the bulk solution in radial direction is the predominant process at the low frequencies (about at kHz). Meanwhile, the M−W−O[42] relaxation (typically at MHz) ascribed to a consequence of an accumulation of polarized charges on the boundary surfaces of dispersed particles.

3.2.2. Dependences of Permittivity Increments on the Volume Fraction. The volume fraction dependences of special dielectric increments of suspensions of PS/PANI particles are shown in Figure 6, where $\partial\varepsilon_l = (\varepsilon_l - \varepsilon_m)/\phi$ and $\partial\varepsilon_h = (\varepsilon_m - \varepsilon_h)/\phi$ denoting the low- and high-frequency relaxation amplitude of suspensions of particles per unit volume, respectively. From this figure, it can be observed that both $\partial\varepsilon_l$ and $\partial\varepsilon_h$ are increasing with the enhancement of ϕ, which is not consistent with the predictions of theory proposed by Delgado et al.,[49] meanwhile, it has contradiction with the dielectric analysis for suspensions of polystyrene and palladium nanoparticle chains.[49,51,52] Otherwise, this analyzing result is consistent with the results concluded from suspensions of PS/PPY[32] and PS/ZnO[33] microspheres, separately. Considering that the results of previous studies on the dielectric relaxation,[49,51,52] increasing the particle concentrations will reduce the effective charges of particle surface due to the mutual overlap of electrical double layer of particles, furthermore, both $\partial\varepsilon_h$ mainly ascribed to the smaller counterion concentration in the diffuse layer and then $\partial\varepsilon_l$ due to a relatively smaller ion concentration gradient in the adjoining

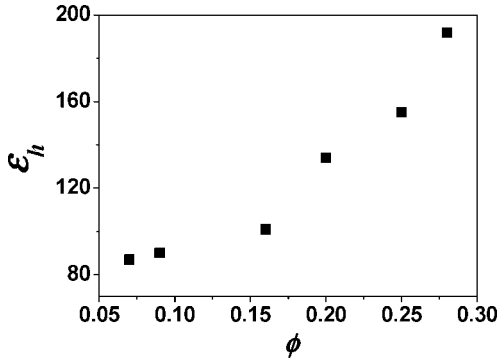

Figure 7. Dependence of the high-frequency permittivity (ε_h) on the volume fraction of PS/PANI particles.

bulk solution, are decreasing with the increment of ϕ, just as concluded from some former works. [49,51,52] Therefore, we supposed that except for the effect of counterion atmosphere the relaxation amplitude of this system is mainly determined by the electric feature of PS/PANI(PPY, ZnO) core−shell particles themselves since only two main factors, the counterion atmosphere near particles and the self-characteristic of particles, can affect relaxation amplitude. The common element of these three suspensions of PS/PANI, PS/PPY and PS/ZnO is the PS core is nonconducting, the shell (PPY, PANI and ZnO) is conducting. Therefore, we can gain a conclusion from the elucidative point of dielectric analysis induced from the prediction of O'Brien on dielectric response of a dilute suspension of semiconducting particles,[53] that is except for the two typical relaxations—the low- and high-frequency relaxations which occurred at lower frequencies (kilohertz) and higher frequencies (megahertz), respectively, suspensions exhibit an additional dielectric relaxation over the megahertz frequency field, here named "the third relaxation", due to the polarization of internal double layer of the thin layer of conducting PANI, PPY and ZnO when an external field is employed, just as that concluded in our previous paper. [33]

3.2.3. Dependence of the High-Frequency Permittivity on the Volume Fraction. Figure 7 shows the dependence of high-frequency permittivity ε_h on the volume fraction of PS/PANI particles dispersed in 0.05 mM KCl electrolyte solution. As for the analysis of this figure, it looks like an easy way, otherwise we can conclude two distinct and important results: the first is the high-frequency permittivity ε_h is increased with the volume fraction of PS/PANI particles, and the other is each of ε_h for suspensions of PS/PANI microspheres is higher or much higher than the permittivity of aqueous solution (80.05 at 18 ± 1 °C).

For analyzing the results clearly, now we introduce the interfacial polarization theory presented first by Maxwell[46] and developed by Wagner,[41] then we can obtain the equation

$$\varepsilon_h = \varepsilon_m\left(1 + 3\varphi\frac{\varepsilon_p - \varepsilon_m}{2\varepsilon_m + \varepsilon_p}\right) \quad (7)$$

where ε_m and ε_p are the permittivity of aqueous solution and particles, respectively.

Equation 7 indicates that when $\varepsilon_p \leq \varepsilon_m$ (most systems belong to this case, including our PS/PANI system, as we well-known the permittivity of conducting or nonconducting polymer is in the range of 2−10), the high-frequency permittivity ε_h of high-frequency relaxation is decreased with the increment of ϕ, meanwhile, each ε_h of suspensions should be lower than the permittivity (80.05 at 18 ± 1 °C) of aqueous solution (disperse medium), namely, the fact should be $\varepsilon_h \leq \varepsilon_m \approx \varepsilon_{H_2O}$ (80.05).

However, as for our complex system—suspension of PS/PANI microspheres, both of the results obtained in our experimental data are opposite to the fact that has been considered correct for a long time. Facing this embarrassment, we have compared this phenomenon with the dielectric analysis deduced from suspensions of classical particles PS,[49,52] the PS/PPY[32] and PS/ZnO[33] microspheres. The contrastive result is: the dielectric characteristic of suspensions of PS/PANI microspheres is coincident with the dielectric analysis of suspensions of PS/PPY, and has contradiction with that of PS/ZnO micrespheres. First, we suppose that the reason resulting in this unusual phenomenon is the high-frequency relaxation associated with the interfacial polarization is unfinished in MHz frequency field, namely, the two interfaces of PANI/solution and PS/PANI are existed in structure of PS/PANI, which will result in two M−W relaxations caused by two consequent interfacial polarizations. Meanwhile, these two polarized processes are so close to each other that these two relaxations of interfacial polarization are overlapped and can not be distinguished, distinctly. On the other hand, we can understand it from the elucidative point of dielectric analysis induced from the prediction of O'Brien on dielectric response of a dilute suspension of semiconducting particles,[53] suspensions exhibit an additional dielectric relaxation over the megahertz frequency field due to the polarization of internal double layer of the thin layer of conducting PANI when an external field is employed, it indicates that the polarized ramification of internal double layer deduced from the additional relaxation has worked on the high-frequency of M−W interfacial relaxation. Therefore, the additional relaxation is responsible for the unusual ε_h of suspensions. In conclusion, no matter which explanation, structure and electric characteristic of the additional PANI shell are responsible for this special dielectric behaviors of suspensions of PS/PANI core−shell microspheres under the employment of the AC electric field.

Second, based on the dielectric analysis of suspensions of PS/ZnO composite particles,[33] the ε_h data displayed in Table 2 of ref 33 show $\varepsilon_h \leq \varepsilon_m$, and the ε_h value of high-frequency relaxation is decreased with the increment of ϕ, which is in good agreement with the prediction of eq 7 in M−W theory. It indicates that the special ε_h values of the high-frequency relaxation of core−shell composite suspensions are a consequence of the different conducting mechanism and surface morphology of PANI and ZnO shells although they are both conducting materials which can result in the additional relaxation under the AC electric field. As is known, the conducting mechanism of conducting polymer is the electron movement within delocalized π-band orbits and positive charge defects known as polarons and bipolarons [54,55] rather than n-type conductivity with the electrons moving in the conduction band as the charge carriers. [56] The second reason is the PS/PANI (PS/PPY) surface has the large charge storage capability which is originated from PANI (PPY) shell with the porous morphology that allows excellent ions access in three dimensions and its continuous conducting network.[57,58] We should point out that the conducting PANI (PPY) shell with porous morphology is heterogeneous phase, then an accumulation of counter-ions at the interfaces of PS/PANI (PPY) and PANI (PPY)/solution contributes the conductivity and permittivity of dispersed particles.

Therefore, except for the dependences of both $\partial\varepsilon_l$ and $\partial\varepsilon_h$ of suspensions of PS/PANI (PS/PPy and PS/ZnO) core−shell composite microspheres on ϕ are special, the dependence of high-frequency permittivity values ε_h for suspensions of PS/

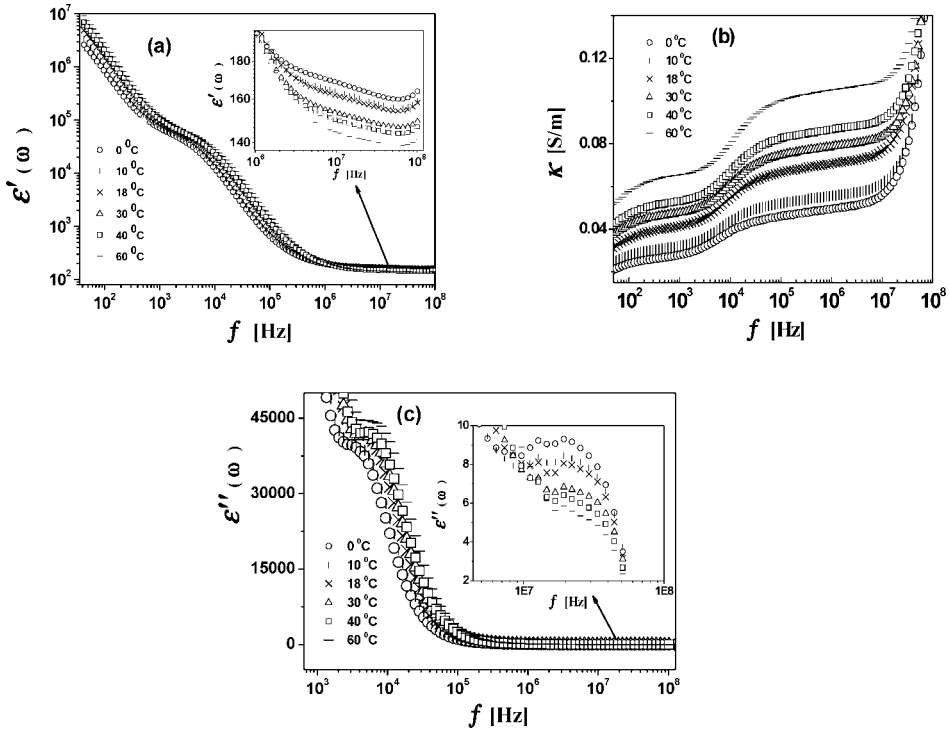

Figure 8. Permittivity ε' (a) and conductivity κ (b) and dielectric loss ε'' (c) of suspensions as a function of the frequency ω of the applied field, for suspensions of PS/PANI core−shell particles with different temperatures indicated.

TABLE 2: Dielectric Parameters of Suspensions of PS/PANI Core−Shell Microspheres with the Indicated Temperatures from 0 to 60 °C

	dielectric parameters							
temperature (°C)	ε_l	ε_m	ε_h	$\Delta\varepsilon_l$	$\Delta\varepsilon_h$	κ_l (S/m)	τ_l[s] (× 10^5 s)	τ_h[s] (× 10^9s)
0	41941	169	156	41772	13	0.0277	2.7322	6.4716
10	43840	163	153	43677	10	0.0318	2.5076	6.2165
18	48650	159	152	48491	7	0.0412	2.1105	6.1900
30	49000	150	145	48850	5	0.0475	1.9056	5.9629
40	49556	145	142	49411	3	0.0527	1.7964	5.9629
60	52600	139	137	52461	2	0.0651	1.4623	5.7583

PANI and PS/PPY particles on the volume fraction are special as well due to its unique conducting mechanism and surface structure.

3.3. Dielectric Relaxation of Suspensions of PS/PANI Particles Dispersed in Electrolyte Solution with Different Temperatures. As we expected that permittivity measurements will eventually be useful as a tool for the electrokinetic study of suspensions, where monodispersity in size and shape is always the main concern. Nevertheless, in other electrokinetic phenomena, temperature acts on the electrokinetic behavior of suspensions of particles through changing the viscosity and dielectric constant of the dispersion medium. Here, we make an effort to outline the salient electrokinetic features (double electric layer/dielectric property) of suspensions of PS/PANI core−shell microspheres under different temperatures by means of the dielectric analysis of dielectric relaxation spectroscopy. In order to realize this dream, we have carried out the dielectric measurements for suspensions of PS/PANI composite microspheres in 0.05 mM KCl solution under various temperatures as indicated, and the experimental results are shown in Figure 8.

Figure 8 shows the dependence of permittivity (a), conductivity (b) and dielectric loss (c) on the frequency ω of the applied field for suspensions of PS/PANI core−shell particles with different temperatures (0−60 °C), individually. First of all, from Figure 8 it can be observed the dependence of ε' at low and high frequencies on temperature of suspensions is different from each other, therefore, which is necessary to explain: first, at high frequencies, the permittivity of PS/PANI suspension decreases when the temperature is raised, as shown in the amplificatory picture of top right corner, which is in good agreement with the well-known behavior of the permittivity of water[59] (78.54 at 25 °C), its permittivity at other temperatures can be obtained by eq 8 (the error is ±0.03%), separately,

$$\varepsilon_t = 78.4[1 - 4.579\times10^{-3}(t-25) + 1.19\times10^{-5}(t-25)^2 - 2.8\times10^{-8}(t-25)^2] \quad (8)$$

where $\varepsilon_{t(w)}$ denotes the permittivity of water (aqueous solution) at arbitrary temperature t_w.

Second, the permittivity of suspension at low frequencies increases when the temperature is raised, which shows the dependence of ε' on temperature of suspensions of PS/PANI particles is absolutely different with that at high frequencies. Considering this phenomenon, we can not help imaging that the contribution of dispersed particles to dielectric behavior of suspensions is most significant at low frequencies since the dependence of ε' on T is not in agreement with the well-known behavior of aqueous solution. For further investigation, the Cole−Cole formula with two- relaxation terms and electrode polarization term, is used to fit the experimental data, then the

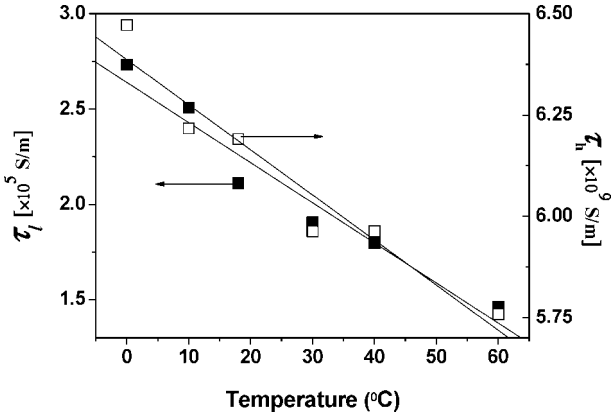

Figure 9. Low- (■) and high-frequency (□) relaxation times plotted as a function of temperature of suspensions of PS/PANI particles, respectively.

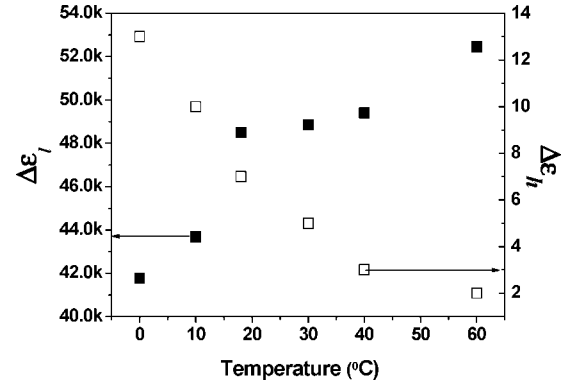

Figure 10. Dielectric increments of the low- (■) and high-frequency (□) relaxations plotted as a function of temperature for suspensions of PS/PANI composite microspheres, respectively.

dielectric parameters are obtained and the best-fitting results are listed in Table 2.

As a consequent investigation, the dependence of relaxation time and some dielectric parameters on the temperatures will be displayed and discussed in detail in the following paragraphs, one by one.

3.3.1. Dependence of the Characteristic Relaxation Time on Temperature of Suspensions. Figure 9 shows the dependence of low- (τ_l) and high-frequency (τ_h) relaxation time on temperatures (10−60 °C) of suspensions of PS/PANI microspheres, which exhibits that both τ_l and τ_h decrease with the increment of temperature. As for the field changes direction in the time $2\pi/\omega$ (counterion relaxation), the counter-ions at low frequencies (typically at kHz) can effectively move from one side of the particle to the other, a distance of ca. $2(a + \chi^{-1})$. Then, at high frequencies (typically at MHz), ions of the double layer can only shake back and forth in electric double layer, that is, $\langle x \rangle \approx \chi^{-1}$.

Therefore, the relaxation time of the low- and high-frequency relaxations can be respectively estimated by

$$\tau_l \approx \frac{4(a+\chi^{-1})^2}{2D} \tag{9}$$

$$\tau_h \approx \frac{\chi^{-2}}{2D} \tag{10}$$

The Debye length or the double layer thickness χ^{-1} [60,61] can be expressed as

$$\chi^{-1} = \sqrt{\frac{\varepsilon_0 \varepsilon_e k_B T}{2e^2 C_\infty}} \tag{11}$$

$$D(=k_B T/\lambda) \tag{12}$$

Where D is the diffusion coefficient of counterion and λ its drag coefficient, k_B the Boltzmann constant, T the absolute temperature (291 ± 1 °C). From eqs 9 and 10, we can conclude that two elements contribute to the characteristic relaxation time (τ_l and τ_h): one of which is $D(=k_B T/\lambda)$, and the other is the double layer thickness, χ^{-1}. Therefore, the discussion on the dependence of τ_l and τ_h on temperature is based on the two directions in the following section. According to eq 12, D is increased with increasing temperature, this is originated from the ease of ionic transport due to the decrease in the viscosity of the liquid medium (that is the decrease of its drag coefficient, λ), on the other side, χ^{-1} is increased with the increment of temperature on the basis of eq 11. Then, one picture comes into our mind for our system under investigation, that is a significant decrease of characteristic relaxation time (both τ_l and τ_h) with increasing temperature as shown in Figure 9. Thus, we can make it clear that, the predominant element of contributing the dielectric process of suspension is the faster transport of counter-ions, which is ascribed to the increment of the diffusion coefficient of counterion when the temperature of suspensions of PS/PANI particles increases.

In conclusion, "which element is predominant in dielectric relaxation process" is depended on the competitive result between the increasing magnitude of the double layer thickness and the counterion mobility. For our PS/PANI system, the act of temperature on the dielectric behavior of suspensions is mainly resulting from the counterion mobility due to the decrease of viscosity of liquid medium.

3.3.2. Dependence of Dielectric Increment on the Temperature of Suspensions. Figure 10 shows the dependence of dielectric increments of the low- ($\Delta\varepsilon_l$) and high-frequency ($\Delta\varepsilon_h$) relaxations on the temperatures (0−60 °C) of suspensions of PS/PANI microspheres, individually. It is shown that when the temperature (T) of suspensions of PS/PANI microspheres raises, $\Delta\varepsilon_h$ is decreased, on the contrary, $\Delta\varepsilon_l$ shows the increasing dependency on the increment of temperature. Prior to giving the explanation of this phenomenon, we will recall the evolution of related investigation for the dependence of dielectric behavior of particle suspensions on the temperatures where the particles existed. Recently, Arroyo[62] has investigated the effect of temperature and polydispersity on the dielectric relaxation of dilute Ethylcellulose suspensions, which shows that amplitude of the dielectric relaxation decreases when temperature is raised. This agrees qualitatively with predictions based on the classical electrokinetic theory proposed by DeLacey and White.[29] The dielectric behaviors of suspensions of PS particles in different experiment temperatures have been investigated as well by Jiménez et al.,[63,64] combining the dielectric relaxation and electrophoretic mobility of colloid suspensions at different temperatures.

Here, with the aim of improving this description, we make an attempt to explain the dependence of the low-frequency dielectric increments on temperature of PS/PANI suspensions. As we known that for the low-frequency dielectric relaxation there are two mechanisms which are currently used to explain the low-frequency (kHz range) dielectric relaxations (LFDR) of permittivity of suspensions. This has resulted in the development of two alternative models: the first, the surface diffusion mechanism (SDM) proposed by Schwarz,[45] is associates the LFDR with the diffusion of bound ions along the particle surface

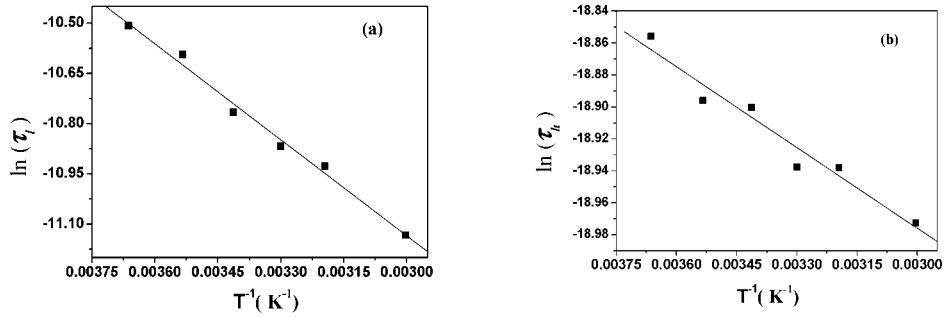

Figure 11. Plots of ln τ against $1/T$: (a) low-frequency relaxation and (b) high-frequency relaxation, individually.

caused by the applied electric field. The second, the volume diffusion mechanism (VDM) proposed by Dukhin and Shilov,[24] follows from the generalization for alternating fields of the classical theory of the relaxation effect in electrophoresis and associates the LFDR with the diffusion of free ions in the diffuse double layer. Now we will analyze it in the following paragraph, one by one. First, for SDM model: the static dielectric increment is expressed as

$$\Delta\varepsilon_l = \frac{9}{4}\frac{4\pi\varphi}{\left(1+\frac{\varphi}{2}\right)^2}\frac{e_0^2 a\sigma_0}{k_B T} \tag{13}$$

Where ϕ is volume fraction, $e_0$is the electrical mount of electron, σ_0 is charge intensity of particle surface at equilibrium state, k_B is the Boltzmann constant, T is absolute temperature, a is the radius of particle. The formula followed from the SDM establishes the relation between the low-frequency dielectric increment ($\Delta\varepsilon_l$) and temperature in the Schwarz model, in which it shows that when temperature raises the $\Delta\varepsilon_l$ should decreases. Recalling the results shown in Figure 10, $\Delta\varepsilon_l$ is increased with the increment of temperature of suspensions of PS/PANI microspheres, therefore, the mechanism of low-frequency relaxation of PS/PANI suspensions belongs to the VDM model rather than the SDM model. Then, the dielectric increment of VDM model is described as

$$\frac{\Delta\varepsilon}{\varepsilon_m} = \frac{9}{4}\varphi(\chi a)^2\frac{(A_1a_2 - A_2a_1)(1+W+W^2)}{(A_1+A_1W)^2+(A_1W+A_2W^2)^2} \tag{14}$$

In the expression of eq 14, A_1, A_2, a_1, and a_2 are associated with counterion valence, ion strength and zeta potential; a is the radius of PS/PANI particles; W is associated with the strength of applied electric field, and ionic diffusion coefficient which is associated with temperature of suspensions. The Debye length or the double layer thickness χ^{-1} has been expressed in eq 11. Equations 11 and 14 establish the relation between the low-frequency dielectric increment ($\Delta\varepsilon_l$) and temperature in the VDM model developed by Dukhin and Shilov,[24] in which it shows three contributions (the ionic diffusion coefficient, the double layer thickness χ^{-1} and zeta potential) are responsible for the dielectric behaviors when the temperature of PS/PANI suspensions raises. These contributions should be further differentiated, the χ decreases according to eq 11 and will result in the decrement of $\Delta\varepsilon_l$ when temperature of suspensions increases. Otherwise, the results shown in Figure 10, $\Delta\varepsilon_l$ is increased with the increment of temperature of suspensions, therefore, two elements are responsible for the increasing of $\Delta\varepsilon_l$ when temperature increases, which is the faster mobility of transferring counter-ions and the larger zeta potential, then we should point out the faster mobility of transferring counter-ions are the main element just as concluded in Section 3.3.1. Second, the dependence of high-frequency dielectric increments on temperature is impressed in my mind, as shown in Figure 10, $\Delta\varepsilon_h$ is decreased when the temperature of suspensions increases. Although discussions on the dielectric behavior of suspensions are so few except for the investigation reported by Jiménez,[63,64] here we confirm that the dependence of $\Delta\varepsilon_{h(\mathrm{MWO})}$ on temperature of suspensions is qualitatively coincident with the prediction of standard electrokinetic theories and the results obtained from the dielectric study of suspensions of PS particles, as demonstrated in investigation. [63]

The following physical arguments can be given to the different dependences of the magnitude for the low- and high-frequency relaxations on temperature as well. When T rises, the low-frequency conduction current decreases, which is usually presented as the increment of dielectric increment ($\Delta\varepsilon_l$) in dielectric property of suspensions. The reason for this is the counter-ions at low frequencies will move from one side of the particle to the other, and the hindrance and collision of mutual ions in such long distance is increased with the increment of temperature. As a result, the magnitude of low-frequency conduction current is decreased with the increment of temperature. Meanwhile, when T rises, the high-frequency conduction current increases(presented as the decrease of dielectric increment ($\Delta\varepsilon_h$)) as a consequence of the faster motions of ions due to less hindrance and collision of mutual ions in such short distance of electrical double layer when the ac applied electric field. Therefore, the dependences of dielectric increments of low- and high-frequency relaxations on temperature are different from each other although both of them are due to the decreasing of the viscosity and the permittivity of disperse medium.

3.3.3. Determination of Activation Energy of the Relaxation Process. Relaxation phenomena are controlled by thermally activated kinetics, namely, the lowest limiting energy caused the occurrence of dielectric relaxation. The evaluation of activation energy is traced back to the energy E_a in the Arrhenius formula $\kappa = Ae^{-E_a/RT}$ where κ is reaction rate, so E_a is called the Arrhenius activation energy and it is defined as experimental activation energy since it is obtained from experimental data—reaction rate constants κ at several temperatures. Then we will obtain the dependence of κon T from the plots of lnκ against $1/T$, correspondingly, the activation energy of the relaxation process (E_a) can be obtained from the slop ($-E_a/R$) of the fitting line where $R = 8.314$ J/(mol·K) (gas constant). Therefore, here an Arrhenius expression is used to describe the dependence of the dielectric relaxation time on the relaxation temperature of PS/PANI particles. For the low- and high-frequency relaxations, ln τ is plotted against $1/T$ as shown in Figure 11a and b, individually. Each plot is well expressed by a linear equation

$$\ln \tau = \ln \tau_0 + \frac{E_a}{R}\frac{1}{T} \quad (15)$$

According to the Figure 11, we can obtain

$$\ln \tau_l = -14.0029 + 955.92 \times \frac{1}{T} \quad (16)$$

for the low-frequency relaxation,

$$\ln \tau_h = -19.4820 + 168.65 \times \frac{1}{T} \quad (17)$$

for the high-frequency relaxation.

From eqs 16 and 17, the activation energies E_a of the characteristic relaxation progress at low (kHz) and high (MHz) frequencies are determined as $E_{al} = 7.947 \times 10^3$ J/mol and $E_{ah} = 1.402 \times 10^3$ J/mol, individually, and here we defined them as the lowest limiting energy for the occurrence of low- and high-frequency relaxations, separately. Therefore, here the activation energy of the low- and high-frequency relaxations of suspensions of PS/PANI microspheres has been experimentally determined by the dielectric data, separately. Meanwhile, the result shows the occurrence of low- and high-frequency relaxations is much easier than chemical reaction since most of the energy of chemical reaction has been determined and confirmed in the range of 40−400 kJ/mol.

4. Conclusion

The main focus of the present work is concerned with discovering the dielectric behavior of PS/PANI originated from the effect of volume fraction and temperature on dielectric relaxation of suspensions of PS/PANI composite microspheres over a frequency range of 40 Hz to 110 MHz.

On the basis of the comparisons of dielectric parameters of suspensions of PS/PANI and PS, PS/PPY, and PS/ZnO particles, there are five significative phenomena have been extracted from the dielectric analysis, which are defined as a consequence of the special dielectric behavior of suspensions of PS/PANI core−shell microspheres under ac applied fields. First, an abnormal phenomenon, namely, special dielectric increments, where $\partial\varepsilon_l = (\varepsilon_l - \varepsilon_m)/\phi$ and $\partial\varepsilon_h = (\varepsilon_m - \varepsilon_h)/\phi$ denoting the low- and high-frequency relaxation amplitude of suspensions of PS/PANI particles per unit volume, respectively, are increasing with the enhancement of volume fraction, ϕ. Second, the high-frequency permittivity (ε_h) presented in dielectric parameters is higher or even much higher than 80.05 (18 ± 1 °C)—the permittivity of aqueous solution. Both of them indicate that except for the two distinct relaxations—the low- and high-frequency relaxations, respectively, PS/PANI suspensions exhibit an additional dielectric relaxation over the megahertz frequency range, here named "the third relaxation", due to the polarization of internal double layer of the thin layer of conducting polymer PANI when ac field is employed. Meanwhile, dependences of $\varepsilon_h$on ϕ are different for suspensions of PS/PANI(PS/PPY) and PS/ZnO particles, which indicates that the special ε_h values of PS/PANI(PS/PPY) suspensions of core−shell composite microspheres are a consequence of the different conducting mechanism and surface morphology of PANI(PPY) and ZnO shell. Third, the low-frequency dielectric relaxation is dominated by the volume diffusion mechanism (VDM) deduced from dependences of both the low-frequency relaxation time (τ_l) on volume fraction and the low- frequency dielectric increment ($\Delta\varepsilon_l$) on temperature of PS/PANI suspensions. Fourthly, on the basis of dependences of dielectric parameters of the low- and high-frequency relaxations on the temperature of suspensions, the dielectric behavior of suspension is strongly affected by the increment of transport mobility of counterion due to the decrease of the viscosity of the liquid medium. Finally, according to the copy of an Arrhenius expression, the activation energies of the low- and high-frequency dielectric relaxations of suspensions of PS/PANI microspheres have been obtained by the dielectric data, experimentally.

In conclusion, the contribution of new data and analysis on dielectric behaviors of suspensions of nonconducting/conducting polymers composite microspheres, is presented again. The performance presented in this article is a demonstration of special dielectric behaviors of PS/conducting polymer composite microspheres with the unique interfacial property.

Acknowledgment. This work is financially supported by the National Nature Science Foundation of China (no. 20673014). We also show grateful thankfulness to the Ying Chu group of department of chemistry Northeast Normal University, Changchun, 130024, P. R. China, for guiding us to synthesize the PS/PANI microspheres.

References and Notes

(1) Mathew, R. J.; Yang, D. L.; Mattes, B. R. *Macromolecules* **2002**, *35*, 7575.
(2) Wei, Z. X.; Zhang, Z. M.; Wan, M. X. *Langmuir* **2002**, *18*, 917.
(3) Huang, J.; Virji, S.; Weiller, B. H.; Kaner, R. B. *J. Am. Chem. Soc.* **2003**, *125*, 314.
(4) Anand, J.; Palaniappani, S.; Sathyanarayana, D. N. *Prog. Polym. Sci.* **1998**, *23*, 993.
(5) Somani, P. R. *Mater. Chem. Phys.* **2002**, *77*, 81.
(6) Ghosh, P.; Siddhanta, S. K.; Haque, S. R.; Chakrabariti, A. *Synth. Met.* **2001**, *123*, 83.
(7) Caruso, F. *Adv. Mater.* **2001**, *13*, 11.
(8) Khan, A.; Armes, S. P. *Adv. Mater.* **2000**, *12*, 671.
(9) Lascelles, S. F.; Armes, S. P. *J. Mater. Chem.* **1997**, *7*, 1339.
(10) Barthet, C.; Armes, S. P.; Lascelles, S. F.; Luk, S. Y.; Stanley, H. M. E. *Langmuir* **1998**, *14*, 2032.
(11) Han, M. G.; Armes, S. P. *Langmuir* **2003**, *19*, 4523.
(12) Li, Y.; Neoh, K. G.; Kang, E-T. *J. Colloid Interface Sci.* **2004**, *275*, 488.
(13) Wiersma, A. E.; vd Steed, L. M. A.; Jongeling, T. J. M. *Synth. Met.* **1995**, *71*, 2269.
(14) Mangeney, C.; Bousalem, S.; Connan, C.; Adenier, A.; Baunier, P.; Chehimi, M. M. *Langmuir* **2006**, *22*, 10163.
(15) Lyklema, J. *" Fundamentals of Interface and Colloid Science*; Academic Press: London, 1995; Vol. II, p 3208.
(16) Dukhin,S. S.; Derjaguin, B. V. In *Surface and Colloid Science*; Matijevič, E., Ed.; Wiley: New York, 1974; Vol. 7.
(17) O'Brien, R. W.; White, L. R. *J. Chem. Soc. Faraday Trans.* **1978**, *2* (74), 1607.
(18) DeLacey, E. H. B.; White, L. R. *J. Chem. Soc. Faraday Trans.* **1981**, *2* (77), 2007.
(19) Schwan, H. P.; Schwarz, G.; Maczuk, J.; Pauly, H. *J. Phys. Chem.* **1962**, *66*, 2626.
(20) Dunstan, D. E.; White, L. R. *J. Colloid Interface Sci.* **1992**, *152*, 308.
(21) Carrique, F.; Zurita, L.; Delgado, A. V. *J. Colloid Interface Sci.* **1994**, *166*, 128.
(22) Gittings, M. R.; Saville, D. A. *Langmuir* **1995**, *11*, 798.
(23) Arroyo, F. J.; Delgado, A. V.; Carrique, F.; Jiménez, M. L.; Bellini, T.; Mantegazza, F. *J. Chem. Phys.* **2002**, *114*, 10973.
(24) Dukhin,S. S.; Shilov, V. N. *Dielectric Phenomena and the Double Layer in Disperse Systems and Polyelectrolytes*; Wiley: New York, 1974.
(25) O'Brien, R. W. *Adv. Colloid Interface Sci.* **1982**, *16*, 281.
(26) Lyklema, J.; Dukhin, S. S.; Shilov, V. N. *J. Electroanal. Chem.* **1983**, *143*, 1.
(27) Grosse, C.; Foster, K. R. *J. Phys. Chem.* **1987**, *91*, 3073.
(28) Shilov, V. N.; Delgado, A. V.; González- Caballero, F.; Grosse, C. *Colloids Surf., A* **2001**, *192*, 253.
(29) Mangelsdorf, C. S.; White, L. R. *J. Chem. Soc. Faraday Trans.* **1997**, *2* (93), 3145.
(30) López-García, J. J.; Horno, J.; Delgado, A. V.; González-Caballero, F. *J. Phys. Chem. B* **1999**, *103*, 11297.
(31) Dukhin, S. S. *Adv. Colloid Interface Sci.* **1993**, *44*, 1.

(32) Han, M. J.; Zhao, K. S.; Zhang, Y. P.; Chen, Z.; Chu, Y. *Colloids Surf., A* **2007**, *302*, 174.
(33) Han, M. J.; Zhao, K. S. *J. Phys. Chem. C* **2008**, *112*, 9192.
(34) Yang, Y.; Chu, Y.; Zhang, F. Y. *Mater. Chem. Phys.* **2005**, *92*, 164.
(35) Hanai, T.; Zhang, H. Z.; Sekine, K.; Asaka, K.; Asami, K. *Ferroelectrics* **1988**, *86*, 191.
(36) Ishikawa, A.; Hanai, T.; Koizumi, N. *Jpn. J. Appl. Phys.* **1981**, *20*, 79.
(37) Asami, K.; Irimajiri, A.; Hanai, T.; Koizumi, N. *Bull. Inst. Chem. Res., Kyoto Univ.* **1973**, *51*, 231.
(38) Cole, K. S.; Cole, R. H. *J. Chem. Phys.* **1941**, *9*, 341.
(39) Hanai, T.; Imakita, T.; Koizumi, N. *Colloid Polym. Sci.* **1982**, *260*, 1029.
(40) Asami, K. *Prog. Polym. Sci.* **2002**, *27*, 1617.
(41) Wagner, K. W. *Arch. Elektrotech. (Berlin)* **1914**, *2*, 371.
(42) O'Konski, C. T. *J. Phys. Chem.* **1960**, *64*, 605.
(43) Jiménez, M. L.; Arroyou, F. J.; Turnhout, J. V.; Delgado, A. V. *J. Colloid Interface Sci.* **2002**, *249*, 327.
(44) Wübbenhorst, M.; Turnhout, J. V. *Dielectrics Newsletter* **2000**, *1*−*6*, 1956.
(45) Schwarz, G. *J. Phys. Chem.* **1962**, *66*, 2636.
(46) Maxwell, J. C. *A Treatise on Electricity and Magnetism*, 3rd ed.; Clarendon Press: Oxford, 1891; Chapter 4.
(47) Shilov, V. N.; Borkovskaya, Y. B. *Koiloiidn. Z.* **1994**, *56*, 647.
(48) Borkovskaya, Y. B.; Shilov, V. N. *Koiloiidn. Z.* **1992**, *54*, 43.
(49) Delgado, A. V.; Arroyo, F. J.; González-Caballero, F.; Shilov, V. N.; Borkovskaya, Y. B. *Colloids Surf., A* **1998**, *140*, 139.
(50) Shilov, V. N.; Delgado, A. V.; González-Caballero, F.; Horno, J.; López-García, J. J.; Grosse, C. *J. Colloid Interface Sci.* **2000**, *232*, 141.
(51) Chen, Z.; Zhao, K. S. *J. Chem. Phys.* **2007**, *126*, 164505.
(52) Barchini, R.; Saville, D. A. *J. Colloid Interface Sci.* **1995**, *173*, 86.
(53) O'Brien, R. W. *J. Colloid Interface Sci.* **1996**, *177*, 280.
(54) Waller, A. M.; Compton, R. G. *J. Chem. Soc. Faraday Trans.* **1989**, *185* (4), 977.
(55) Dong, S.; Ding, J.; Zhan, R. *J. Chem. Soc. Faraday Trans.* **1989**, *185* (7), 1599.
(56) Bundesmann, C.; Schubert, M.; Spemann, D.; Butz, T.; Lorenz, M.; Kaidashev, E. M.; Grundmann, M.; Ashkenov, N.; Neumann, H.; Wagner, G. *Appl. Phys. Lett.* **2002**, *81*, 2376.
(57) Ghosh, S.; Inganas, O. *Adv. Mater.* **1999**, *11*, 1214.
(58) Fusalba, F.; Belanger, D. J *Phys. Chem. B* **1999**, *103*, 9044.
(59) *Handbook of Chemistry and Physics*, 66th ed.; CRC Press: Boca Raton, FL, 1985.
(60) Dukhin, S. S. *Adv. Colloid Interface Sci.* **1995**, *61*, 17.
(61) Tirado, M.; Grosse, C. *J. Colloid Interface Sci.* **2006**, *298*, 973.
(62) Arroyo, F. J.; Carrique, F.; Delgado, A. V. *J. Colloid Interface Sci.* **1999**, *217*, 411.
(63) Jiménez, M. L.; Arroyo, F. J.; Carrique, F.; Kaatze, U.; Delgado, A. V. *J. Colloid Interface Sci.* **2005**, *281*, 503.
(64) Jiménez, M. L.; Arroyo, F. J.; Carrique, F.; Delgado, A. V. *J. Colloid Interface Sci.* **2007**, *316*, 836.

JP803530M